Engineering Failure Analysis 167 (2025) 109066

Contents lists available at ScienceDirect

Engineering Failure Analysis

journal homepage: www.elsevier.com/locate/engfailanal

Surface analysis of bilateral tibial inserts retrieved due to polyethylene wear and PCL-deficiency

N. Hidayah [a], S. Liza [a,*], A.M. Merican [b], A.A. Abbas [b], K.A. Ayob [b]

[a] TriPreM i-Kohza, Department of Mechanical Precision Engineering, Malaysia-Japan International Institute (MJIIT), Universiti Teknologi Malaysia, 54100 Kuala Lumpur, Malaysia

[b] National Orthopaedic Centre of Excellence in Research and Learning (NOCERAL), Department of Orthopaedic Surgery, Faculty of Medicine, University of Malaya, 50603 Kuala Lumpur, Malaysia

ARTICLE INFO

Keywords:
Tibial insert
Polyethylene
Wear
Oxidation
Posterior cruciate ligament

ABSTRACT

This paper investigates the surface damage modes found on bilateral tibial inserts (implanted for 137 and 146 months). This paper also investigated whether posterior cruciate ligament (PCL) deficiency can be considered an external factor that worsen wear and contribute towards total knee replacement (TKR) failure. Results show that pitting, scratching, and delamination were the dominant wear features on both inserts and surface roughness was higher on lateral compartments of both inserts. PCL deficiency contributed towards increased surface roughness in the medial compartment of the left insert but was not the main factor leading to TKR failure. The right insert showed oxidation index (OI) of 1.57, crystallinity of 88.95 %, microhardness of 5.55 ± 0.82 HV, and molecular weight of 30,975 g/mol. Meanwhile, the left insert exhibited OI of 2.99, crystallinity of 60.89 %, microhardness of 5.51 ± 1.51 HV, and molecular weight of 295,246 g/mol. Our study concludes that long-term implantation leads to more severe oxidation degradation of the inserts.

1. Introduction

Total knee replacement (TKR) is a surgical procedure widely used for treating severe knee arthritis to relieve pain and improve function in patients with advanced joint disease. However, the need for revision surgeries due to primary TKR failure remains a concern, with the failure rate at around 6 % at 12 years post-operatively [1]. Recent studies found that the major causes of implant failure are instability, alongside infection, aseptic loosening, stiffness, and polyethylene wear [2,3].

The primary cause of polyethylene wear in TKR was a combination of persistent oxidative degradation and mechanical stress, with the former expediting the latter [4]. Oxidative degradation had been shown to worsen over longer implantation time [5], resulting in changes in mechanical properties thus leading to further mechanical degradation. Previous failure analysis studies categorized wear features into two groups: low-grade wear (burnishing, abrasion, and cold flow) and high-grade wear (scratching, pitting, metal embedding, and delamination) [6]. High-grade wear, such as delamination, has been found in short (<5 years), medium (5–10 years), and long (>10 years)-term retrievals [7].

On the other hand, previous literature reviews reported that 32 % of patients complained of knee instability accompanied by pain and limited activity [8]. This factor is more common in knee replacement compared to hip replacement due to the relatively flat knee

* Corresponding author.
E-mail address: shahiraliza@utm.my (S. Liza).

https://doi.org/10.1016/j.engfailanal.2024.109066
Received 24 March 2024; Received in revised form 24 October 2024; Accepted 9 November 2024
Available online 12 November 2024
1350-6307/

tibial surface as opposed to the ball-in-socket shape of the hip joint, which allows for a greater range of motion and a higher degree of conformity between the articulating surfaces, resulting in smoother movement and reduced wear [9]. Instability can be explained as abnormal displacement of the knee prosthesis, resulting in clinical failure [10]. Late instability after TKR can be caused by either polyethylene wear alone or coupled with the integrity of surrounding ligaments, such as the posterior cruciate ligament (PCL) [10]. Previous studies have shown that PCL deficiency after primary TKR often results in instability thus leading to revision surgeries [11].

The bilateral tibial inserts in this study were retrieved due to wear (right insert) and PCL deficiency (left insert) which may lead to instability. Therefore, this surface analysis study was done to explain the degradation that occurred during in vivo service and to understand the impact of long-term implantation and whether PCL deficiency will influence surface damage in any way. These inserts were retrieved from a senior female patient's bilateral knee prostheses. Microscopy, spectroscopy, calorimetry, and microhardness were implemented to gain information on the physical, chemical, and mechanical properties and degradation after their in vivo service.

2. Materials and methods

2.1. Retrieved samples

The study investigated bilateral UHMWPE tibial inserts retrieved from a 75-year-old female patient who initially underwent primary bilateral knee replacement surgery in September 2007. Approximately a decade following surgery, the patient began to experience significant pain in both knees, exacerbated by movement and particularly acute during walking and directional changes. The pain was more pronounced on the right side. Clinical evaluations revealed no signs of effusion or fluid accumulation around either implant. The narrow gap between the tibial and femoral components, as marked by red arrows and lines in the radiographic analysis in Fig. 1, indicated a reduction in insert thickness in both left and right tibial inserts pre-explantation. However, there was no loosening of the implant-bone interface or misalignment occurred. The explanted prostheses were identified as cruciate-retaining conventional UHMWPE models (NRG-Stryker), designed without the inclusion of a post.

2.1.1. Right-knee

The right knee implant was retrieved in February 2019, 11 years and 5 months after implantation. Mild coronal plane instability was detected, but the range of motion remained within acceptable limits, and the PCL was intact. The revision procedure showed no signs of loosening of the metal components, so only the UHMWPE tibial insert was replaced. Notable wear patterns were identified on the insert's medial and lateral articulating surfaces.

2.1.2. Left-knee

The left knee implant was removed in November 2019 after 12 years and 2 months of implantation. The clinical assessment found more looseness in the front-to-back direction of the joint, which led to the joint bending backward more than normal. While the metallic components of the implant remained securely fixed, the PCL was deficient. Thus, the metal component was removed alongside the tibial insert to accommodate a posterior-stabilized implant system.

2.2. Surface evaluation (zoning)

The failure analysis of retrieved UHMWPE tibial inserts was performed by examining the surface morphology of the samples. This study focused on the UHMWPE inserts used in knee joint applications, specifically looking at the interface between the femoral metal and the polymer tibial insert. Over extended years of use, these inserts underwent noticeable changes in their surface characteristics. This analysis aimed to evaluate the alterations in surface roughness and degradation of the UHMWPE samples, primarily attributed to wear-related activities during their in vivo service.

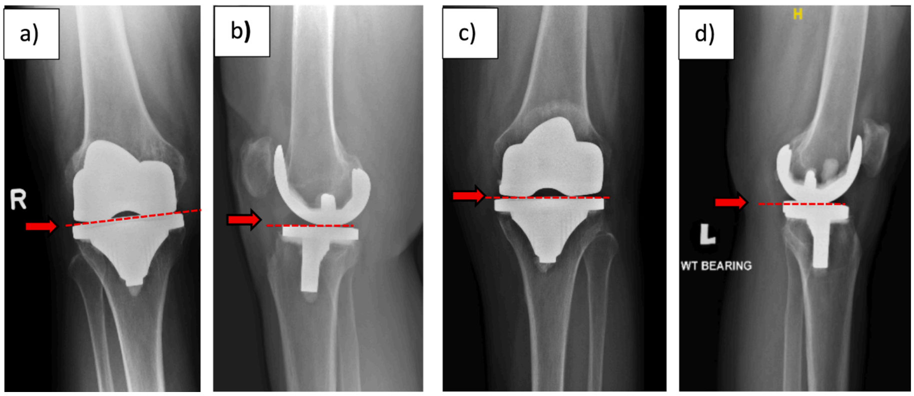

Fig. 1. Radiographs pre-explantation of right knee a) front, b) lateral and left knee c) front, d) lateral.

Surface analysis was done according to a zoning pattern used by Currier et.al [12] that built upon Wasielewski et al's works. The grid used in this study divided the sample into three zones (top, middle, bottom) for each medial–lateral compartments and a zone between the medial–lateral compartments, as shown in Fig. 2. 3D Digital Microscope (Hirox, USA Inc.) was utilized to assess wear degradation on the retrieved samples. This approach is expected to identify areas with higher surface roughness, indicative of wear damage. Surface roughness was then quantitatively measured using a 3D Optical Surface Profiler (ZeGage, ZYGO, United States). Multiple measurements were recorded at various points within each zone. The average values from these measurements were compared between the left and right UHMWPE inserts and across different zones on the medial–lateral side.

Additionally, high-resolution 3D imaging gave detailed information about the surface profile of each measured area. Subsequently, these identified areas will be examined in greater detail using a Scanning Electron Microscope (SEM) (JOEL JSM-6010 Plus/LV) to characterize the wear damage further, focusing on areas with pronounced surface roughness in both the medial and lateral compartments for the left and right knee inserts.

2.3. Oxidation characterisation

It has been observed that oxidation in Ultra-High Molecular Weight Polyethylene (UHMWPE) can lead to a deterioration in its mechanical characteristics, such as a reduction in toughness and a decline in wear resistance, which ultimately contributes to the material's degradation [13,14]. Attenuated Total Reflection-Fourier Transform Infrared Spectroscopy (ATR-FTIR) (IRTracer-100 Fourier Transform Infrared Spectrometer) was employed to measure the extent of oxidative degradation in UHMWPE samples. This technique involved analyzing the strength of the carbon–oxygen bonds. The analysis targeted the bulk region of the tibial inserts. The samples' thickness varied within a flexible range to ensure firm contact with the ATR crystal, which is critical for accurate readings. The scanning spectrum captured transmittance data ranging from 500 cm^{-1} to 4000 cm^{-1}. The Oxidation Index (OI) was calculated by comparing the area under the carbonyl peak around 1700 cm^{-1} with a reference peak between 1330 cm^{-1} and 1390 cm^{-1} as shown by the Equation (1) below:

$$\text{Oxidation Index (OI)} = \frac{A_{\text{carbonyl}}}{A_{\text{reference}}} \tag{1}$$

Equation (1): Oxidation index calculation [15]

2.4. Crystallinity measurement

The degree of crystallinity in UHMWPE is directly related to its mechanical strength and stiffness. A higher crystallinity usually translates to increased hardness and wear resistance but can also lead to decreased toughness [16]. The crystalline regions provide structural stability, while the amorphous regions allow for some flexibility. The degree of crystallinity was measured using Differential Scanning Calorimetry (DSC) (Shimadzu DSC 60 Plus Standard model) by quantifying the heat of fusion needed to melt the polymer [17]. The sample weight used was 5 mg, and the analysis was performed by purging nitrogen gas at a flow rate of 10 mL/minute. The sample was then heated with an initial temperature of 30 °C at a rate of 10 °C/minute until it reached the final temperature of 250 °C and subsequently kept at a constant temperature for 5 min before it was cooled down to 5 °C. The sample was kept at a constant temperature for 5 min and then reheated back to 250 °C at the same rate as previously stated. The percentage of crystallinity was measured by comparing the total heat of melting to the total heat of fusion. The initial heat of fusion for UHMWPE is 239 J/g [16].

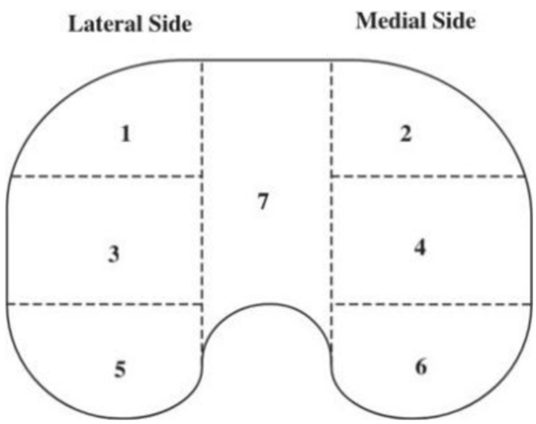

Fig. 2. The grids used to divide the implant into zones for surface analysis [12].

2.5. Molecular weight measurement

UHMWPE's high molecular weight contributes significantly to its exceptional mechanical properties. The long polymer chains increase entanglement, enhancing the material's toughness and impact resistance. Higher molecular weight UHMWPE also tends to have better wear resistance, which is crucial for applications like joint replacements [18]. Gel Permeation Chromatography (GPC) is a well-established technique for separating and determining molecular weights of polymers, including UHMWPE. It provides valuable data on the molecular weight changes due to mechanical degradation, oxidation, or other factors affecting the polymer's integrity [19]. This measurement was performed by GPC (Waters 2414 refractive index (RI) detector, Gentech Scientific, New York) analysis on selected zones of the retrieved UHMWPE samples with recorded mass of 0.1 g. The UHMWPE samples were thinly sliced and dissolved in Tetrahydrofuran at approximately 60 °C for seven days. The weight average molecular weight (Mw) and number average molecular weight (Mn) were used to calculate the polydispersity index (PDI), which is defined as PDI = Mw/Mn [20].

2.6. Microhardness test

Microhardness is a mechanical test conducted to measure the hardness of the retrieved tibial insert at the microscopic level. This test is commonly used in failure analysis studies of retrieved tibial inserts as it can provide valuable information about the material properties and potential causes of failure [21–23,6]. A small indenter is pressed into the surface of the material being tested during a microhardness test. A load of 98 mN was applied with a holding time of 15 s. The size and shape of the indentation were used to calculate the material's hardness as shown in Fig. 3. The equation for Vickers hardness (Hv) is shown below:

$$H_v = 1854.4\left(\frac{P}{d^2}\right)\text{kgf mm}^{-2} \tag{2}$$

Equation (2): Equation for Vickers hardness [24]

3. Results and discussion

There were a few limitations that should be acknowledged. Firstly, the authors had no access to the patient's full medical history before revision surgery. Secondly, the original specifications of the UHMWPE tibial insert preceding implantation, such as its original dimensions, mechanical and chemical properties, were unavailable. As such, this lack of knowledge prohibited authors from proposing an in-depth relationship between underlying medical conditions and the state of the retrieved implant. Instead, this study will focus on analyzing the bilateral tibial inserts' surface damage and establishing the relationship, if any, between surface damage observed and uneven load distribution due to instability under the influence of PCL integrity combined with the long-term implantation service. The 11 years 5 months right tibial insert's and 12 years 2 months left tibial insert's in vivo service in this study provided a realistic representation of the mechanical loads and oxidative degradation that the tibial inserts underwent in the knee joint and therefore offered valuable insights into the long-term performance of the implant.

UHMWPE tibial inserts from the bilateral knee prosthesis were received in a condition with significant damage on both right and left inserts. General visual observation showed that the 11 years 5 months right tibial insert which was retrieved due to wear had more severe macroscopic surface damage than the 12 years 2 months left tibial insert which was retrieved due to PCL deficiency. Previous research has indicated that a lack of PCL may lead to instability, which is hypothesized to alter the load distribution on the knee and influence the wear patterns of the polyethylene material in the implant [25,26]. In contrast, the normal PCL-intact knee is expected to maintain more stable biomechanics with high-grade wear and oxidative degradation, as previously found in long-term failure analysis studies [27]. The consistent compressive strain in PCL-intact knee contributes towards the more significant macro damage of the right knee [28]. Thus, further analysis on a microscopic level was done to characterise the damage and confirm whether PCL integrity played any role in the observed surface damage.

The inserts were analysed according to Currier zoning system [12]. There was visible damage in the middle zone of both lateral-medial compartments of the right and left tibial insert, as shown in Fig. 5 and Fig. 4, as expected due to the distribution of Von Mises (effective) stress on the surface of the tibial insert during normal knee joint movement which is concentrated at the middle zone [29].

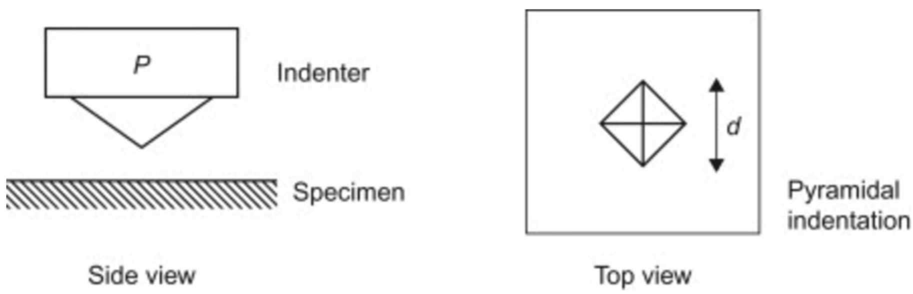

Fig. 3. Schematic of microhardness indentation [24].

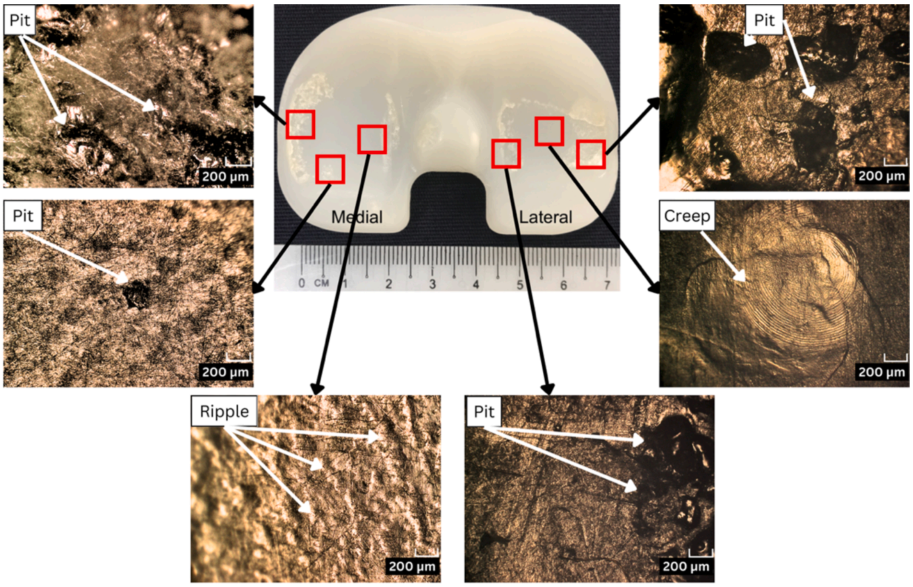

Fig. 4. Wear modes found using 3D digital microscope on middle zone of the right tibial inserts medial compartment and lateral compartments.

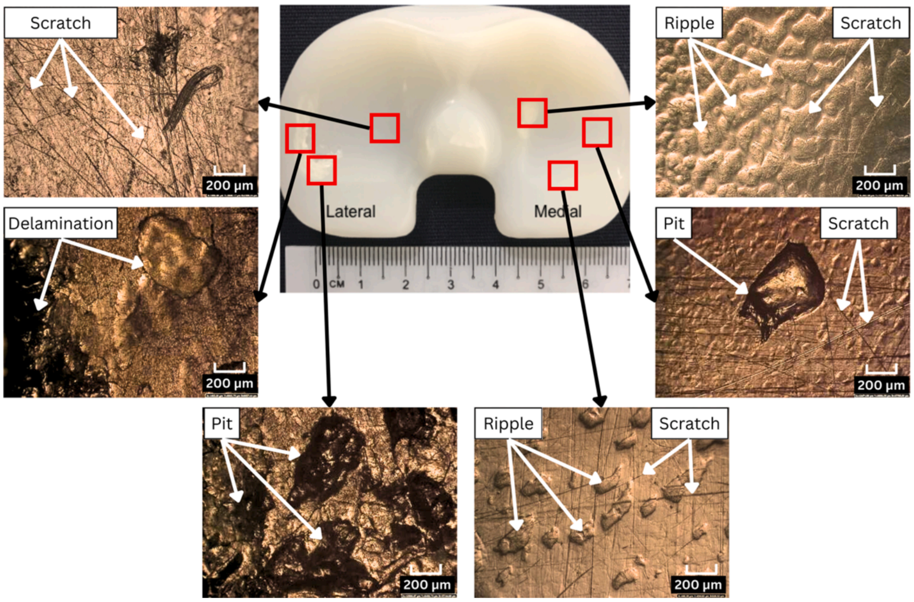

Fig. 5. Wear modes found using 3D digital microscope on middle zone of the left tibial inserts medial compartment and lateral compartments.

This stands true regardless of the knee implant designs as supported by previous studies [12,30] and a more recent computational model that showed wear concentrated in the middle zone of the tibial insert [31]. The retrieved tibial inserts' conditions were further analyzed by characterizing the morphological conditions. 3D optical microscope images of the 11 years 5 months right tibial insert in Fig. 4 revealed small craters, known as pits, as the dominant wear modes found alongside patterns of deformation, recognized as creep and ripple wear. On the other hand, microscopic analysis of the 12 years 2 months left tibial insert's surface recorded multidirectional scratches and pits of various sizes in both medial and lateral compartments as shown in Fig. 5. Notably, the lateral compartment showed onset of delamination with visual signs of the polyethylene layer separation. In contrast, the medial compartment was distinguished by a rippled, bumpy texture indicative of surface deformation. From these micrographs' observation, the surface wear damage on the 12 years 2 months left tibial insert from mechanical loading were less severe which can be contributed to the PCL-deficiency induced instability, which can lead to altered gait characteristics and joint contact mechanics, thus affecting the distribution of contact loads on the implant surface [32,33].

To further understand the extent of surface damage observed, surface roughness measurements of the retrieved tibial inserts were performed. The average surface roughness data in Table 1 showed a significant difference between the lateral-medial part for both right and left tibial inserts. The average surface roughness of the lateral part (5.753 ± 18.37) μm was higher than the medial part (3.863 ± 10.47) μm for the 11 years 5 months right tibial insert, and a similar trend was observed in the 12 years 2 months left tibial insert where the average surface roughness of the lateral part (5.843 ± 9.10) μm was higher than the medial part (4.181 ± 9.73) μm. The rough surface on the lateral part indicates the surface have undergone more wear than the medial part. The lateral compartment often endures higher mechanical stress during activities as it compensates for gait and weight distribution variances, particularly during dynamic activities such as turning and high flexion activities [26,34]. Additionally, although the dynamic load was higher in the medial compartment, articular cartilage is anatomically thicker in the lateral compartment in both the femur and tibia [35]. These factors could explain the increased wear and surface roughness laterally. The average surface roughness of lateral part of right and left tibial inserts does not differ significantly, suggesting that the integrity of PCL might not significantly alter the distribution of stress across the lateral compartment of the knee [28,36]. However, when examining the medial compartments, the surface roughness values in the PCL-deficient 12 years 2 months left tibial insert are notably higher (4.181 ± 9.73) μm compared to those in the PCL-intact 11 years 5 months right tibial insert (3.863 ± 10.47) μm. Interestingly, an increase in surface roughness values in the bottom region of the PCL-deficient left tibial insert was observed. This finding was supported by Deng et al. who found that PCL deficiency changes the knee joint mechanics and cause instability, particularly evident in the posterior (bottom) region due to the posterior subluxation of the medial tibial plateau [28]. These alterations lead to increased wear and surface damage in the medial compartment of the PCL-deficient 12 years 2 months left tibial inserts, proven by higher surface roughness values compared to the PCL-intact 11 years 5 months right tibial insert.

Further morphological analysis was done to clarify whether the surface damage, in any way, was influenced by knee's PCL integrity and implantation time. 3D laser images in Fig. 6 (a-b) showed pits and scratches in the PCL-intact 11 years 5 months right tibial insert, with the lateral part showing more severe surface damage than the medial part. Meanwhile, pits and scratches are found on the PCL-deficient 12 years 2 months left tibial insert, with the lateral part showing higher damage than its medial part, as shown in Fig. 7(a-b).

SEM further characterized the surface damage to understand the wear features' occurrence and implantation time. The SEM analysis was performed on the middle zone, with higher surface roughness as more wear features contribute to the high surface irregularities expected to be observed in this zone. The microscopic images of the SEM analysis for the right tibial insert and left tibial insert are shown in Fig. 8 and Fig. 9 respectively. Previous failure analysis studies assessed the retrieved tibial insert for seven modes of surface damage: pitting, scratching, delamination, third body debris, surface deformation, burnishing, and abrasion [37] to determine the severity of surface damage. The SEM analysis revealed that delamination was the dominant wear mode across the lateral-medial compartment of the right tibial insert with clear evidence of material detachment and pit formation, as illustrated in Fig. 8 (b-d). Scratches were also present, as shown in Fig. 8 (a,f). Other wear features observed were creep in Fig. 8(a) and ripples in Fig. 8 (e), characterized by its wave-like appearance and prominent only on the medial part.

On the other hand, the SEM analysis of the left tibial insert found that multidirectional scratch tracks are prominent across the lateral-medial part, evidenced in Fig. 9 (a-f). At the same time, delamination was more dominant on the lateral part, as shown in Fig. 9 (a-c). Fig. 9 (b,d,f) showed pitting was found on the lateral-medial part of the left tibial insert. Like the right tibial insert, the left tibial insert also possessed ripples only on its medial part, as indicated in Fig. 9 (d-f).

Delamination refers to separating large sheets of polyethylene from the underlying layers. It is typically observed in short (< 5 years), medium (5–10 years), and long (> 10 years) term retrievals of knee prostheses [7]. It is a severe type of wear and is often the result of mechanical fatigue and oxidative degradation over time [38]. While abrasive and adhesive wear mechanisms predominantly characterize retrieved acetabular hip liners, fatigue-worn surfaces are more commonly observed in knee tibial inserts [3,39]. Fatigue in this context is defined as the progressive and localized micro-structural damage occurring from cyclic loading, with the 'fatigue life' being the number of cycles needed to reach catastrophic material failure. It has been reported in previous studies that conventional polyethylene has a fatigue life of approximately five million cycles, after which fatigue-related wear modes like delamination and pitting become evident [13,39]. Given that the average gait cycle from walking activity of patient with total knee replacement (TKR) is about 1.2 million cycles per year [40], the emergence of delamination and pitting in this study is expected due to the prolonged duration of implantation of 11 years 5 months and 12 years 2 months which surpass the five million cycles threshold [41]. However, as the patient was elderly with a knee condition, the patient may experience lower cyclic loading due to inactivity; thus, cyclic loading might not be the major contributor to the delamination damage. Hence, oxidation may be the main factor leading to delamination damage, which will be further investigated. Previous studies elaborate on this interaction, highlighting the compounded effects of mechanical stress and oxidative processes on the integrity of the polyethylene material in the context of knee joint replacements [13,14,42].

In addition to delamination, scratch tracks and pits were also detected on both tibial inserts' surfaces, often resulting from the

Table 1
Surface roughness measurement of bilateral UHMWPE tibial inserts.

PE Tibial Insert	Compartment Zone	Top 1,2	Middle 3,4	Bottom 5,6	Average (μm)
Right	Lateral	5.012 ± 0.45	11.204 ± 18.16	1.043 ± 2.75	5.753 ± 18.37
	Medial	1.432 ± 0.51	8.693 ± 10.38	1.464 ± 1.27	3.863 ± 10.47
Left	Lateral	3.207 ± 2.98	11.879 ± 8.46	2.441 ± 1.50	5.843 ± 9.10
	Medial	2.859 ± 3.14	7.021 ± 7.02	2.664 ± 2.48	4.181 ± 9.73

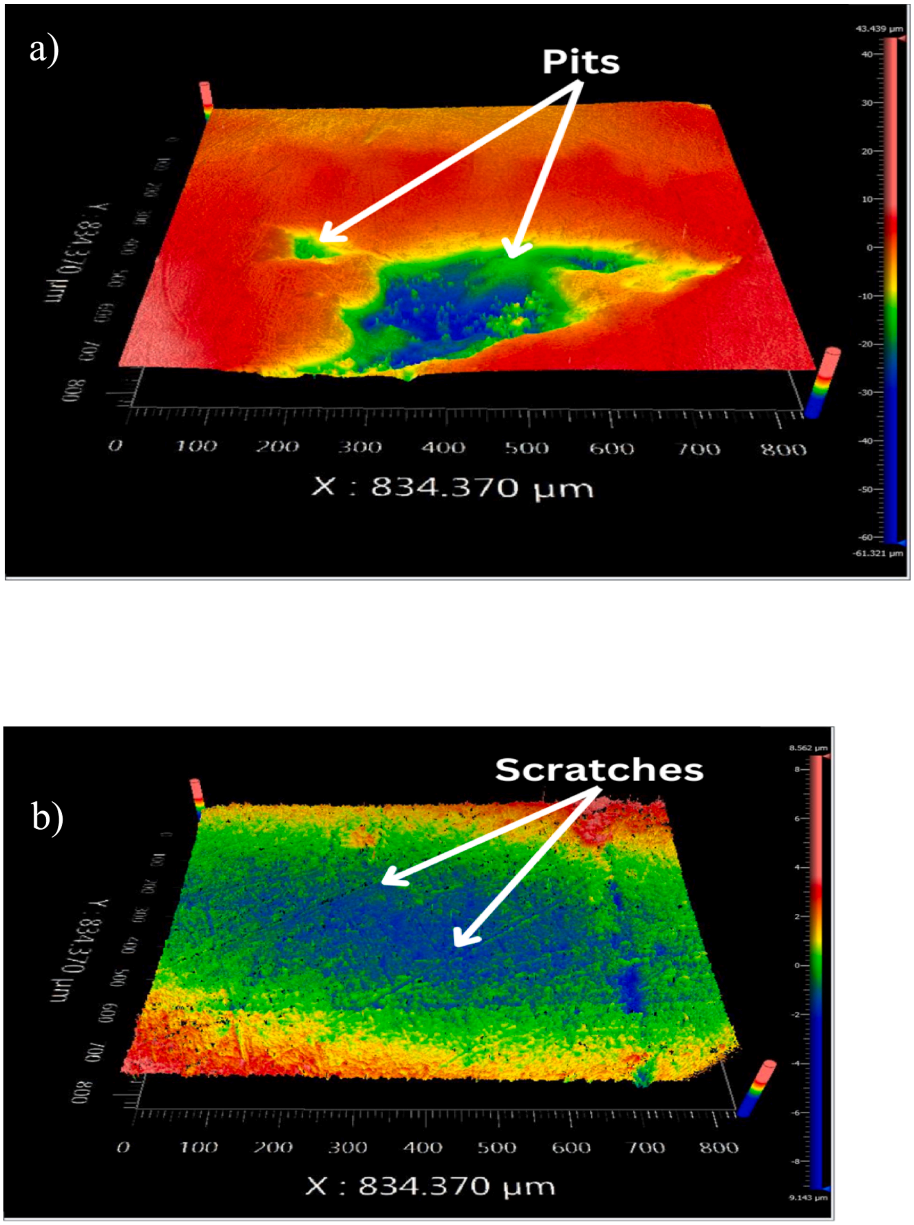

Fig. 6. 3D laser images taken for surface roughness measurement of right knee tibial inserts; a) lateral and b) medial compartment.

abrasive action of particulate debris entering the joint space. A study by Garabedian et al. analyzed the wear pattern on a retrieved tibial insert and found that debris like bone, bone cement, and metallic particles are responsible for third-body abrasion of the polyethylene mobile bearing surface [43]. These particles can drag across the surface of the polyethylene inserts, leading to scratching, defined as hard particles' linear abrasion, or marking of the surface. The contrast in scratch track patterns between the left and right tibial insert showed that the PCL influences stress distribution and subsequent wear patterns across the tibial insert. These findings support the hypothesis that the PCL deficiency resulted in inconsistent kinematics, leading to non-uniform scratches [44,45]. In comparison, the intact PCL stabilizes, thus promoting even stress distribution across the tibial insert surface, reflected in the more consistent scratch track pattern [46]. On the other hand, pitting was characterized by small, round indentations on the articulating surface caused by the same type of abrasive action. Both scratching and pitting can increase the surface roughness of the inserts, potentially leading to higher contact stresses and contributing to the formation of microcracks [47].

Ripples were observed on the medial part of both right and left tibial insert. This wear feature indicated significant alterations to the UHMWPE structure, which suggested irreversible alterations exceeding the yield strength without removing material but may potentially expedite implant failure [48]. This is consistent with our previous finding that the medial part of the tibial inserts showed less damage than the lateral part. The wear mechanisms that control the formation of ripples are not well understood, but it has been

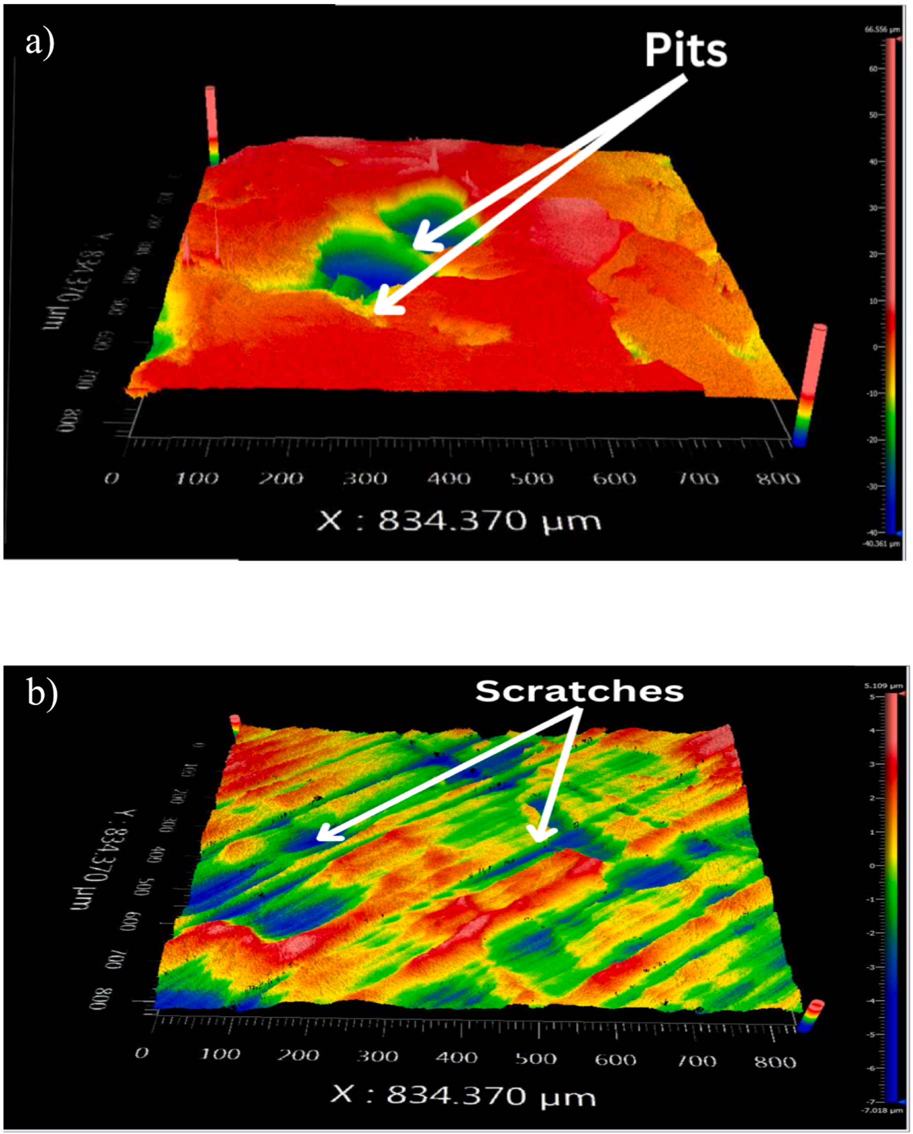

Fig. 7. 3D laser images taken for surface roughness measurement of PCL-deficient left knee tibial inserts; a) lateral and b) medial compartment.

suggested that the ripple formation is associated with fatigue wear and strain-hardening mechanisms in the UHMWPE surface layer [49]. Creep was also observed in right tibial insert and usually caused by progressive and time-dependent deformation of the UHMWPE under sustained loads. This behavior is well-documented in polyethylene components subjected to the repetitive loading and compressive strain like in knee joint dynamic of PCL-intact knee [14,28,42,50].

The surface damage analysis in this study observed delamination, pitting, and scratching as the dominant wear modes found on the lateral-medial part of both right and left tibial insert. A study by Liza et al. (2011) on a retrieved UHMWPE tibial insert after 10 years of service found that high-grade wear and oxidation degradation were present, with observations of surface delamination, scratch marks, and pitting. These findings support the association of the wear features with oxidative degradation during long-term implantation and the resultant wear mechanisms that contribute to the failure of the tibial insert. Thus, from the surface morphology observation, we conclude that the effect of PCL integrity on wear-induced failure was minimal. Instead, the duration of implantation played a bigger role as there was a difference of 7 months in the duration of implantation of right (11 years 5 months) and left (12 years 2 months) tibial inserts. A previous study has shown that even a short 2-month difference in the duration of implantation can influence the extent of wear and damage observed in knee implants due to the oxidative degradation experienced in vivo [51].

The oxidation process in UHMWPE tibial inserts can happen via residual free radicals within the UHMWPE insert, which act as sites for oxidation, reacting with dissolved oxygen in bodily fluids. Subsequently, another mechanism proposes that free radical species present in synovial fluid can initiate in vivo oxidation. The presence of carbonyl groups in UHMWPE indicates oxidative degradation, with studies suggesting that lipids absorbed from synovial fluid can initiate and accelerate oxidation even without detectable residual

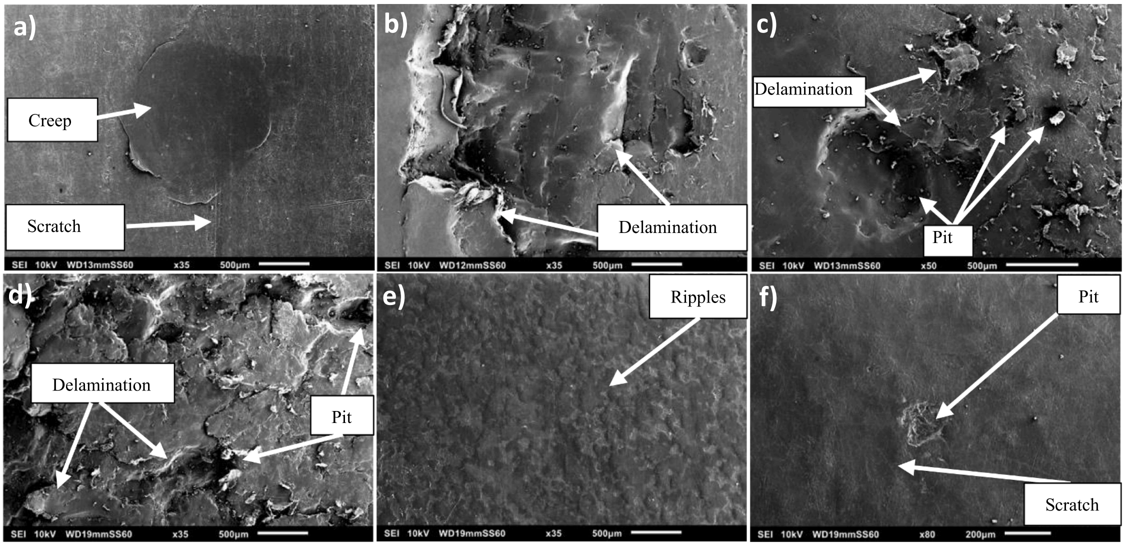

Fig. 8. SEM images for the lateral part (a-c) and medial part (d-f) of the right tibial insert.

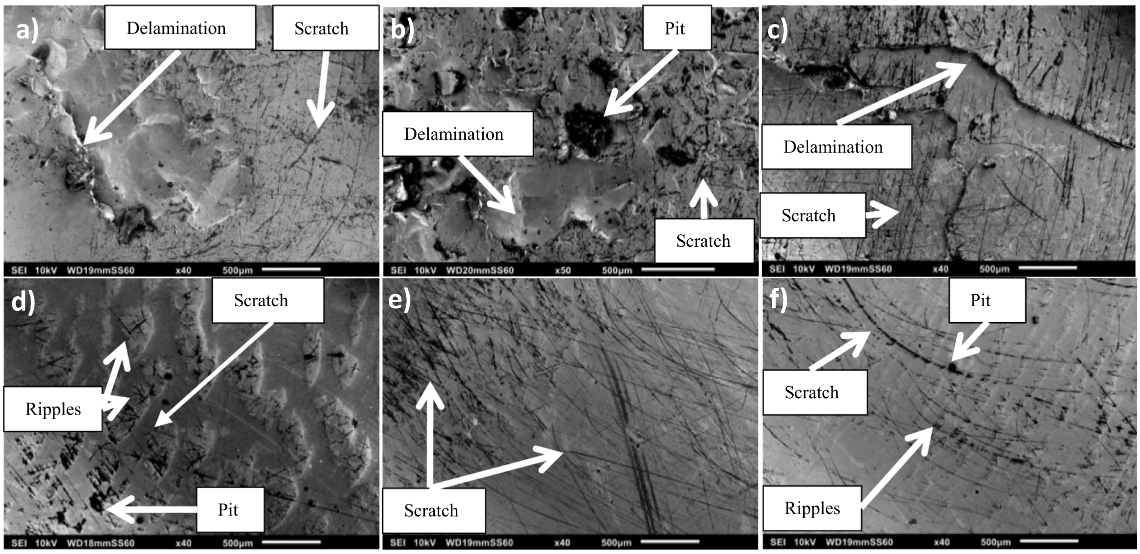

Fig. 9. SEM images for the lateral part (a-c) and medial part (d-f) of the left tibial insert.

free radicals [23,52]. However, identifying the mechanisms involved in in vivo oxidation falls outside the scope of our research. For this study, we will find evidence of oxidation by carbon bonding analysis using ATR-FTIR to correlate its role in inducing mechanical degradation of the implant. Fig. 10 shows the ATR-FTIR for both the right and left tibial inserts, where various absorption bands were identified, signalling the presence of oxidation products. The bands are characterized by specific wavenumbers indicative of different chemical groups: 719 cm^{-1} (C–H bending monosubstituted), 1681 cm^{-1} and 1703 cm^{-1} corresponded to ketone (C = O) and amide (C = O) groups, respectively. The higher carbonyl groups (C = O) bands for the 12 years 2 months left tibial insert suggested a more severe oxidative degradation experienced during the longer implantation duration. The carbonyl groups were formed due to the oxidative degradation of UHMWPE and were a marker of oxidative degradation [53]. The ATR-FTIR spectra analysis confirmed that oxidation had occurred in the bilateral tibial inserts and plays a role towards the degradation of the implant.

The oxidative degradation was further quantified by OI calculation. An OI value below 1 indicates low oxidation, between 1 and 3 signifies moderate oxidation, and values above 3 represent critical oxidation [54]. In this study, the 11 years 5 months right tibial insert had an OI of 1.57, indicating moderate oxidation, while the 12 years 2 months left tibial insert exhibited a higher OI of 2.99, approaching the critical threshold. Oxidation degrades polymer chains, altering the degree of crystallinity and affecting mechanical properties, such as wear resistance and toughness [22]. As seen in conventional UHMWPE explants, the OI tends to increase with longer in vivo periods as seen in the 12 years 2 months left tibial insert, correlating with greater degradation over time.

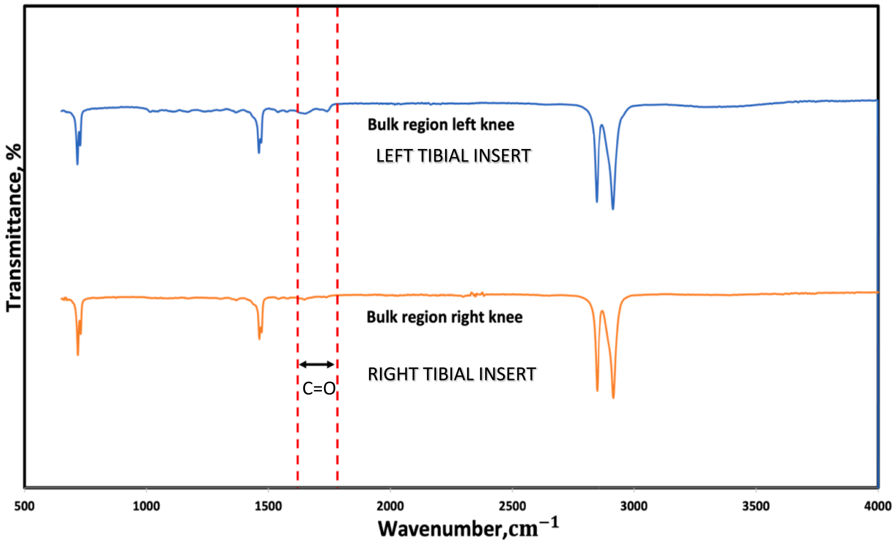

Fig. 10. ATR-FTIR spectra for right and left explanted UHMWPE tibial insert.

To further understand the extent of oxidative degradation, DSC was performed to assess the thermal properties of the tibial inserts after in-vivo service. Fig. 11 shows the degree of crystallinity acquired for both 11 years 5 months right and 12 years 2 months left tibial insert are 88.95 % and 60.29 %, respectively, compared to 100 % crystalline UHMWPE. The crystallinity level was associated with polyethylene's wear resistance. It was notably lower in the 12 years 2 months left tibial insert, indicating a significant degradation of the left insert in the additional 7 months in vivo duration compared to the 11 years 5 months right tibial inserts. This was supported by a previous study that showed significant degradation can occur in a gap as short as 2 months [51]. These findings also aligned with previous studies that have linked lower crystallinity to increased susceptibility to wear and surface damage, including scratching and pitting [18,55,56] and further corroborated our surface analysis in the previous section. At higher crystallinity, the material's structure becomes more organized and tightly structured, which helps to block free radicals from moving around and slows down the material's oxidation process.

The melting temperature for the 11 years 5 months right tibial insert was 139.77 °C, which falls within the typical range for highly crystalline UHMWPE of 130.00 °C – 140.00 °C [57,58]. This suggests that the material's crystalline regions remained well-ordered, requiring significant energy to transition from solid to liquid. Meanwhile, the left tibial insert showed a slightly higher melting temperature of 142.49 °C, likely caused by oxidative cross-linking. Cross-linking increases the energy required for melting, despite the lower crystallinity, by forming additional bonds between polymer chains [59]. In terms of melting temperature range, the 11 years 5 months right tibial insert had a slightly narrower range (20.76°C) compared to 12 years 2 months left tibial insert (21.61 °C). A broader melting range as seen in the 12 years 2 months left tibial insert indicates more amorphous regions, suggesting some loss of structural integrity after prolonged implantation [58,60].

Further analysis of the mechanical degradation was performed through molecular weight measurement through GPC. As shown in Table 2, both tibial inserts experienced significant reduction in molecular weight compared to the medical-grade standard of 1.5 x 10^6 g/mol [50]. The 11 years 5 months right tibial showed a molecular weight reduction of approximately 83.63 % at 245553 g/mol, while the 12 years 2 months left tibial insert exhibited a more severe reduction of 97.94 % at 30975 g/mol, consistent with its longer implantation time [51,61]. Molecular weight reduction due to mechanical stresses and oxidation during in vivo service leads to a decrease in mechanical properties, which can further cause wear and deformation of the tibial insert.

The PDI further highlights these differences: the 11 years 5 months right tibial insert, with a PDI of 1.2, indicates a relatively narrow molecular weight distribution, suggesting minimal degradation and molecular scission during its service life. This aligns with findings that associate a narrower molecular weight distribution in UHMWPE with [21,62]. In contrast, the 12 years 2 months left tibial insert's PDI of approximately 2.3 reflects a broader molecular weight distribution which is often associated with significant oxidative degradation and mechanical stresses. Research has shown that oxidative degradation can lead to an increase in molecular weight variability, which subsequently affects the mechanical performance of UHMWPE [15,62].

A narrow molecular weight distribution, as seen in the 11 years 5 months right tibial insert, is often associated with superior mechanical properties such as tensile strength and wear resistance. Conversely, the broader distribution observed in the 12 years 2 months left tibial insert may compromise mechanical performance, as the presence of lower molecular weight chains increases susceptibility to wear and fatigue [21,62]. These results showed how oxidative degradation altered the molecular structure of UHMWPE tibial inserts, which can affect their long-term performance in vivo.

The mechanical property of the implants was further evaluated through a microhardness test of the tibial inserts. There was a marginal difference in the Vickers Hardness (HV) values, with the 11 years 5 months right tibial insert showing a higher value of 5.55H

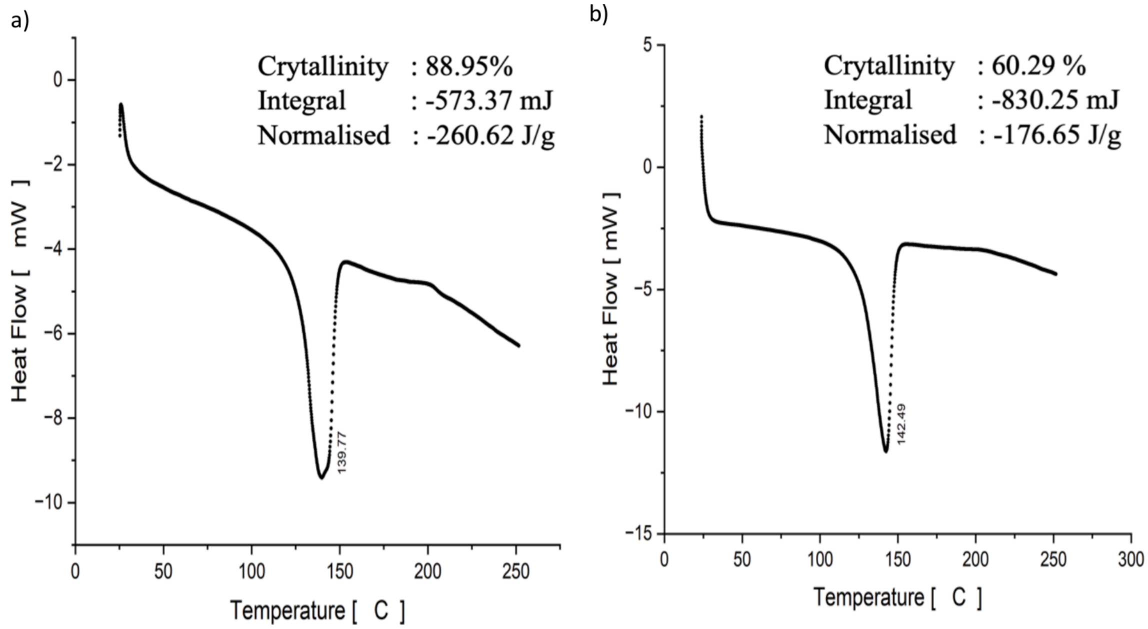

Fig. 11. Heat flow vs temperature for a) right; and b) left UHMWPE tibial inserts.

Table 2
Molecular weight of UHMWPE tibial inserts from GPC analysis.

PE Tibial Insert	Elution volume (ml)	Retention time (min)	Adjusted RT (min)	Mn	Mw [g/mol]	Mp	Mz	MZ + 1
Right	19.167	19.167	19.167	245,553	295,246	295,246	355,469	414,217
Left	24.167	24.167	24.167	13,660	30,975	4978	62,846	87,842

$\pm$ 0.82 HV compared to the 12 years 2 months left tibial insert's hardness of 5.51 $\pm$ 1.51 HV. The microhardness of unused UHMWPE can vary depending on the specific manufacturing process and test conditions. The observed variations in melting temperature and melting range suggested that oxidative degradation was occurring deeper within the material. This degradation was spatially nonuniform, meaning surface hardness measurements may not always capture the full extent of material changes as the subsurface region often experiences more severe degradation [63]. Although surface hardness between both inserts was relatively similar, this underlying degradation can significantly weaken the material over time, thus contributing to the eventual failure of the tibial inserts.

4. Conclusion

This study reveals that the integrity of the posterior cruciate ligament (PCL) impacts the kinematics of the medial compartment, as evidenced by higher surface roughness in the medial compartment of the PCL-deficient left knee. However, PCL integrity is not the primary cause of wear-induced failure in the retrieved tibial inserts, as the major wear modes found in both right and left tibial inserts were identical. The main wear features observed on both the 11 years 5 months right tibial insert and 12 years 2 months left tibial insert were delamination, scratching, and pitting—indicative of oxidation-induced wear surface damage aligned with their long implantation time. Thirdly, the additional 7 months in implantation time had a significant impact on the oxidative degradation of the 12 years 2 months left tibial insert, supported by its lower crystallinity, lower molecular weight, higher PDI and broader melting temperature range. ATR-FTIR analysis confirmed oxidative degradation in both inserts, with higher carbonyl group peaks observed in the left tibial insert, indicating more severe oxidative degradation which was further quantified by OI of 1.57 (11 years 5 months right tibial insert) and 2.99 (12 years 2 months left tibial insert). These findings suggest that oxidation, rather than PCL integrity, is the main contributor to the failure of UHMWPE knee tibial inserts. Surface damage and material changes due to oxidation are significant factors in implant failure, emphasizing the need for enhanced oxidation resistance and mechanical durability in UHMWPE materials for improved longevity of knee prostheses.

CRediT authorship contribution statement

N. Hidayah: Writing – original draft, Investigation. **S. Liza:** Writing – review & editing, Supervision, Conceptualization. **A.M. Merican:** Writing – review & editing, Resources. **A.A. Abbas:** Writing – review & editing, Resources. **K.A. Ayob:** Writing – review &

editing, Resources.

Declaration of competing interest

The authors declare that they have no known competing financial interests or personal relationships that could have appeared to influence the work reported in this paper.

Acknowledgement

This research was financially supported by UTM Fundamental Research grant (Q.K130000.3843.22H20).

Data availability

Data will be made available on request.

References

[1] Y.J. Choi, K.W. Lee, C. Kim, H.S. Ahn, J.K. Hwang, J.S. Kang, H.D. Han, W.J. Cho, J.S. Park, Long-term results of hybrid total knee arthroplasty: minimum 10-years follow-up, Knee Surg Relat Res (2012), https://doi.org/10.5792/ksrr.2012.24.2.79.
[2] M. Pitta, C. Esposito, Z. Li, Y. Lee, T.M. Wright, D.E. Padgett, Failure after modern total knee arthroplasty: a prospective study of 18,065 knees, J. Arthroplasty (2018), https://doi.org/10.1016/j.arth.2017.09.041.
[3] S.M. Kurtz, The Clinical Performance of UHMWPE in Knee Replacements, in: UHMWPE Biomaterials Handbook, Elsevier Inc., 2009: pp. 97–116. https://doi.org/10.1016/B978-0-12-374721-1.00008-0.
[4] J. Gallo, S.B. Goodman, Y.T. Konttinen, M.A. Wimmer, M. Holinka, Osteolysis around total knee arthroplasty: a review of pathogenetic mechanisms, Acta Biomater. (2013), https://doi.org/10.1016/j.actbio.2013.05.005.
[5] H. Fouad, Effect of long-term natural aging on the thermal, mechanical, and viscoelastic behavior of biomedical grade of ultra high molecular weight polyethylene, J. Appl. Polym. Sci. 118 (2010) 17–24, https://doi.org/10.1002/app.32290.
[6] Y. Lu, C.-P. Huang, T.-K. Chang, F.-Y. Ho, C.H. Cheng, Wear-pattern analysis in retrieved tibial inserts of mobile-bearing and fixed-bearing total knee prostheses, J.Bone Joint Surgery - British (2010), https://doi.org/10.1302/0301-620x.92b4.22560.
[7] G.W. Blunn, A.B. Joshi, R.J. Minns, L. Lidgren, P. Lilley, L. Ryd, E. Engelbrecht, P.S. Walker, Wear in retrieved condylar knee arthroplasties: a comparison of wear in different designs of 280 retrieved condylar knee prostheses, J. Arthroplasty 12 (1997) 281–290, https://doi.org/10.1016/S0883-5403(97)90024-3.
[8] C.Y. Li, K.J.N. Cheong Chung, O.M.E. Ali, N.D.H. Chung, C.H. Li, Literature review of the causes of pain following total knee replacement surgery: Prosthesis, inflammation and arthrofibrosis, EFORT Open Rev 5 (2020) 534–543, https://doi.org/10.1302/2058-5241.5.200031.
[9] Hip and Knee Surgery AOA 2022 Report, 2022. www.aoa.org.au.
[10] E.C. Rodriguez-Merchan, Instability following total knee arthroplasty, HSS J. 7 (2011) 273–278, https://doi.org/10.1007/s11420-011-9217-0.
[11] L.B. Moser, P. Prabhakar, S. Hess, M.T. Hirschmann, Diagnostic algorithm in patients with flexion instability after cruciate-retaining total knee arthroplasty: a case report, Clin Pract (2021), https://doi.org/10.3390/clinpract11030084.
[12] J.H. Currier, M.A. Bill, M.B. Mayor, Analysis of wear asymmetry in a series of 94 retrieved polyethylene tibial bearings, J. Biomech. 38 (2005) 367–375, https://doi.org/10.1016/j.jbiomech.2004.02.016.
[13] M. Goldman, M. Lee, R. Gronsky, L. Pruitt, Oxidation of ultrahigh molecular weight polyethylene characterized by fourier transform infrared spectrometry, J. Biomed. Mater. Res. 37 (1997) 43–50, https://doi.org/10.1002/(SICI)1097-4636(199710)37:1<43::AID-JBM6>3.0.CO;2-J.
[14] S.M. Kurtz, W. Hozack, M. Marcolongo, J. Turner, C. Rimnac, A. Edidin, Degradation of mechanical properties of UHMWPE acetabular liners following long-term implantation, J. Arthroplasty 18 (2003) 68–78, https://doi.org/10.1016/S0883-5403(03)00292-4.
[15] L. Zhang, Y. Sawae, T. Yamaguchi, T. Murakami, H. Yang, Investigation on oxidation of shelf-aged crosslinked ultra-high molecular weight polyethylene (UHMWPE) and its effects on wear characteristics, Tribology Online 10 (2015) 1–10, https://doi.org/10.2474/trol.10.1.
[16] S. Hirai, S. Ishimoto, P. Phanthong, S. Yao, Development of surface properties of ultra-high-molecular-weight polyethylene film using side-chain crystalline block copolymers, J. Polym. Eng. (2020), https://doi.org/10.1515/polyeng-2019-0311.
[17] M. Sheng, D. Valco, C. Tucker, E. Cayo, T. Lopez, Practical use of differential scanning calorimetry for thermal stability hazard evaluation, Org. Process Res. Dev. (2019), https://doi.org/10.1021/acs.oprd.9b00266.
[18] Z. Huan, S. Zhao, Z. Xin, C. Ye, Z. Li, J. Xia, Wear resistance mechanism of ultrahigh-molecular-weight polyethylene determined from its structure–property relationships, Ind. Eng. Chem. Res. (2019), https://doi.org/10.1021/acs.iecr.9b04721.
[19] Q. Gu, X. Yi, J. Shen, J. Shi, Y. Liu, J. Shao, A highly automated method for simultaneous determination of sterols, erythrodiol and uvaol in olive oils, Anal. Methods (2016), https://doi.org/10.1039/c6ay00357e.
[20] Polymer Molecular Weight Distribution and Definitions of MW Averages Technical Overview, n.d. www.agilent.com/chem/gpc-sec.
[21] V. Manescu, I. Antoniac, A. Antoniac, G. Paltanea, M. Miculescu, A.I. Bita, S. Laptoiu, M. Niculescu, A. Stere, C. Paun, M.B. Cristea, Failure analysis of ultra-high molecular weight polyethylene tibial insert in total knee arthroplasty, Materials 15 (2022), https://doi.org/10.3390/ma15207102.
[22] B.H. Currier, K.C. Jevsevar, D.W. Van Citters, Oxidation in retrieved, never-irradiated UHMWPE bearings, J. Bone Joint Surgery (American) (2022), https://doi.org/10.2106/jbjs.22.00571.
[23] T. Liu, C. Esposito, J.C. Burket, T.M. Wright, Crosslink density is reduced and oxidation is increased in retrieved highly crosslinked polyethylene TKA tibial inserts, Clin. Orthop. Relat. Res. (2017), https://doi.org/10.1007/s11999-016-4820-5.
[24] R.E. Smallman, A.H.W. Ngan, Characterization and Analysis, in: Modern Physical Metallurgy (Eighth Edition), 2014: pp. 159–250.
[25] J.-A. Lee, Y.-G. Koh, P.S. Kim, K.W. Kang, Y.H. Kwak, K.-T. Kang, Biomechanical effect of tibial slope on the stability of medial unicompartmental knee arthroplasty in posterior cruciate ligament-deficient knees, Bone Joint Res (2020), https://doi.org/10.1302/2046-3758.99.bjr-2020-0128.r1.
[26] G. Li, T.J. Gill, L.E. DeFrate, S. Zayontz, V. Glatt, B. Zarins, Biomechanical consequences of PCL deficiency in the knee under simulated muscle loads—an in vitro experimental study, J. Orthopaedic Research® (2002), https://doi.org/10.1016/s0736-0266(01)00184-x.
[27] S. Liza, A.S.M.A. Haseeb, A.A. Abbas, H.H. Masjuki, Failure analysis of retrieved UHMWPE tibial insert in total knee replacement, Eng. Fail. Anal. 18 (2011) 1415–1423, https://doi.org/10.1016/j.engfailanal.2011.04.001.
[28] Z. Deng, Y. Li, Z. Lin, Y. Zhu, R. Zhao, The biomechanical and histological effects of posterior cruciate ligament rupture on the medial tibial plateau, J. Orthop. Surg. Res. 12 (2017) 48, https://doi.org/10.1186/s13018-017-0551-x.
[29] M.T. Hirschmann, R. Becker, The Unhappy Total Knee Replacement A Comprehensive Review and Management Guide, n.d.
[30] D.C. Grecu, I.V. Antoniac, M. Niculescu, Failure analysis of retrieved polyethylene insert in total knee replacement Dental Biomaterials and Tissue Engineering View project Orthopedic Biomaterials View project, n.d. http://www.revmaterialeplastice.ro.
[31] A. Ozer, Computational wear of knee implant polyethylene insert surface under continuous dynamic loading and posterior tibial slope variation based on cadaver experiments with comparative verification, BMC Musculoskelet. Disord. 23 (2022), https://doi.org/10.1186/s12891-022-05828-2.

[32] J.A. Gustafson, M.E. Robinson, G.K. Fitzgerald, S. Tashman, S. Farrokhi, Knee motion variability in patients with knee osteoarthritis: the effect of self-reported instability, Clin. Biomech. (2015), https://doi.org/10.1016/j.clinbiomech.2015.03.007.

[33] S. Farrokhi, C.A. Voycheck, B.A. Klatt, J.A. Gustafson, S. Tashman, G.K. Fitzgerald, Altered tibiofemoral joint contact mechanics and kinematics in patients with knee osteoarthritis and episodic complaints of joint instability, Clin. Biomech. (2014), https://doi.org/10.1016/j.clinbiomech.2014.04.014.

[34] D. Zhang, S.A. Banks, D.D. D'Lima, C.W. Colwell, B.J. Fregly, In Vivo medial and lateral tibial loads during dynamic and high flexion activities, J. Orthopaedic Research® (2007), https://doi.org/10.1002/jor.20362.

[35] S. Koo, T.P. Andriacchi, A comparison of the influence of global functional loads vs. local contact anatomy on articular cartilage thickness at the knee, J. Biomech. (2007), https://doi.org/10.1016/j.jbiomech.2007.02.005.

[36] C.M. LaPrade, D. Civitarese, M.T. Rasmussen, R.F. LaPrade, Emerging updates on the posterior cruciate ligament, Am. J. Sports Med. (2015), https://doi.org/10.1177/0363546515572770.

[37] R.W. Hood, T.M. Wright, A.H. Burstein, Retrieval analysis of total knee prostheses: a method and its application to 48 total condylar prostheses, J. Biomed. Mater. Res. 17 (1983) 829–842, https://doi.org/10.1002/jbm.820170510.

[38] E. Watanabe, M. Suzuki, K. Nagata, T. Kaneeda, Y. Harada, M. Utsumi, A. Mori, H. Moriya, Oxidation-induced dynamic changes in morphology reflected on freeze-fractured surface of gamma-irradiated ultra-high molecular weight polyethylene components, J. Biomed. Mater. Res. 62 (2002) 540–549, https://doi.org/10.1002/jbm.10357.

[39] O.K. Muratoglu, C.R. Bragdon, M. Jasty, D.O. O'Connor, R.S. Von Knoch, W.H. Harris, Knee-simulator testing of conventional and cross-linked polyethylene tibial inserts, J. Arthroplasty 19 (2004) 887–897, https://doi.org/10.1016/j.arth.2004.03.019.

[40] M. Safaei, R.M. Meneghini, S.R. Anton, Force detection, center of pressure tracking, and energy harvesting from a piezoelectric knee implant, Smart Mater. Struct. (2018), https://doi.org/10.1088/1361-665x/aad755.

[41] C.A. Zahiri, T.P. Schmalzried, E.S. Szuszczewicz, H.C. Amstutz, Assessing activity in joint replacement patients, J. Arthroplasty 13 (1998) 890–895, https://doi.org/10.1016/S0883-5403(98)90195-4.

[42] K. Wannomae, S. Christensen, A. Freiberg, S. Bhattacharyya, W. Harris, O. Muratoglu, The effect of real-time aging on the oxidation and wear of highly cross-linked UHMWPE acetabular liners, Biomaterials 27 (2006) 1980–1987, https://doi.org/10.1016/j.biomaterials.2005.10.002.

[43] C. Garabédian, M. Bigerelle, D. Najjar, H. Migaud, Wear pattern on a retrieved total knee replacement: the "fourth body abrasion,, Biotribology 11 (2017) 29–43, https://doi.org/10.1016/j.biotri.2017.05.003.

[44] D. Wang, J. Graziano, R.J. Williams, K.J. Jones, Nonoperative treatment of PCL injuries: goals of rehabilitation and the natural history of conservative care, Curr. Rev. Musculoskelet. Med. (2018), https://doi.org/10.1007/s12178-018-9487-y.

[45] T.J. Gill, L.E. DeFrate, C. Wang, C.T. Carey, S. Zayontz, B. Zarins, G. Li, The effect of posterior cruciate ligament reconstruction on patellofemoral contact pressures in the knee joint under simulated muscle loads, Am. J. Sports Med. (2004), https://doi.org/10.1177/0095399703258794.

[46] Z. Wang, Y. Xiong, Q. Li, G. Chen, Z. Zhang, X. Tang, J. Li, Evaluation of tibial tunnel placement in single case posterior cruciate ligament reconstruction: reducing the graft peak stress may increase posterior tibial translation, BMC Musculoskelet. Disord. (2019), https://doi.org/10.1186/s12891-019-2862-z.

[47] C.H. Cho, T. Murakami, Y. Sawae, N. Sakai, H. Miura, T. Kawano, Y. Iwamoto, Elasto-plastic contact analysis of an ultra-high molecular weight polyethylene tibial component based on geometrical measurement from a retrieved knee prosthesis, Proc. Inst. Mech. Eng. H (2004), https://doi.org/10.1243/0954411041561018.

[48] J. Nine, D. Choudhury, A.C. Hee, R. Mootanah, N.A. Abu Osman, Wear debris characterization and corresponding biological response, Artificial Hip Knee Joints, Mater. (2014), https://doi.org/10.3390/ma7020980.

[49] J. Wang, Q. Xue, Friction and wear behavior of ultra-high molecular weight polyethylene sliding against GCr15 steel and electroless Ni–P Alloy coating under the lubrication of seawater, Tribol. Lett. (2009), https://doi.org/10.1007/s11249-009-9435-5.

[50] S.M. Kurtz, The UHMWPE Handbook: Ultra-High Molecular Weight Polyethylene in Total Joint Replacement, 2004.

[51] M.Y. Tan, S. Liza, S.M.P. Khadijah, A.A. Abbas, A.M. Merican, K.A. Ayob, N.W.M. Zulkifli, H.H. Masjuki, Surface analysis of early retrieved polyethylene tibial inserts for both knees in total knee replacement, Eng. Fail. Anal. 109 (2020) 104279, https://doi.org/10.1016/j.engfailanal.2019.104279.

[52] E. Oral, B.W. Ghali, A. Neils, O.K. Muratoglu, A new mechanism of oxidation in ultrahigh molecular weight polyethylene caused by squalene absorption, J Biomed Mater Res B Appl Biomater 100 B (2012) 742–751, https://doi.org/10.1002/jbm.b.32507.

[53] I.Y. Grubova, M.A. Surmeneva, V.V. Shugurov, N.N. Koval, I.I. Selezneva, S.M. Lebedev, R.A. Surmenev, Effect of electron beam treatment in air on surface properties of ultra-high-molecular-weight polyethylene, J. Med Biol. Eng. 36 (2016) 440–448, https://doi.org/10.1007/s40846-016-0135-y.

[54] A. Ors-Unsal, V.-M. Archodoulaki, Comparison of in-vivo performance characteristics of first-generation and second-generation cross-linked and conventional explants, J. Arthroplasty 35 (2020) 3330–3337, https://doi.org/10.1016/j.arth.2020.06.012.

[55] A.L. Bruck, K.S. Kanaga Karuppiah, S. Sundararajan, J. Wang, Z. Lin, Friction and wear behavior of ultrahigh molecular weight polyethylene as a function of crystallinity in the presence of the phospholipid dipalmitoyl phosphatidylcholine, J. Biomed. Mater. Res. B Appl. Biomater. (2010), https://doi.org/10.1002/jbm.b.31587.

[56] W. Cui, S. Yang, X. Zhang, Y. Zhang, Y. Shao, X. Li, Y. Bian, X. Weng, S. Xin, J. Zhang, High Wear Resistance of Ultralow-Wear Polyethylene With Different Molecular Weights Under Different Contact Pressure, (2022). https://doi.org/10.21203/rs.3.rs-1286346/v1.

[57] J.M.D. da Silva, S.V.C.R. Coutinho, R.K.M. Diniz, A.N.F. Almeida, M.E.A. Lima, F.de C. Fim, Evaluation of the mechanical and thermal properties of blended (HDPE/UHMWPE) nanocomposites with graphite nanosheets (GNS), Macromol. Symp. 383 (2019), https://doi.org/10.1002/masy.201800017.

[58] Y. Khalil, N. Hopkinson, A. Kowalski, J.P.A. Fairclough, Characterisation of UHMWPE polymer powder for laser sintering, Materials 12 (2019) 3496, https://doi.org/10.3390/ma12213496.

[59] J. Shen, G. Gao, X. Liu, Natural polyphenols enhance stability of crosslinked UHMWPE for joint implants, Clin. Orthop. Relat. Res. 473 (2015) 760–766, https://doi.org/10.1007/s11999-014-3850-0.

[60] V.C. de Souza, J.E. de Oliveira, S.J.G. de Lima, L.B. da Silva, Influence of Vitamin C on morphological and thermal behaviour of biomedical UHMWPE, Macromol. Symp. 344 (2014) 8–13, https://doi.org/10.1002/masy.201300202.

[61] S.M.P. Khadijah, S. Liza, N. Shahemi, A.M. Merican, A.A. Abbas, K.A. Ayob, Surface analysis of retrieved bilateral UHMWPE tibial inserts under varus malalignment condition, Eng. Fail. Anal. 118 (2020), https://doi.org/10.1016/j.engfailanal.2020.104850.

[62] J.-Z. Xu, K.K. Wannomae, O.K. Muratoglu, E. Oral, Increased oxidative protection by high active Vitamin E content and partial radiation crosslinking of UHMWPE, J. Orthopaedic Research® 36 (2018) 1860–1867, https://doi.org/10.1002/jor.23835.

[63] N.H. Shahemi, S. Liza, Y. Sawae, T. Morita, K. Fukuda, Y. Yaakob, The relations between wear behavior and basic material properties of graphene-based materials reinforced ultrahigh molecular weight polyethylene, Polym. Adv. Technol. 32 (2021) 4263–4281, https://doi.org/10.1002/pat.5428.